Self passivating W-based alloys as plasma facing material for nuclear fusion

F Koch and H Bolt

Max-Planck-Institut für Plasmaphysik, EURATOM Association, Boltzmannstr.2, D-85748 Garching, Germany

E-mail: freimut.koch@ipp.mpg.de

Abstract
Self passivating tungsten-based alloys may provide a major safety advantage in comparison with pure tungsten (W) which is presently the main candidate material for the plasma-facing protection of future fusion power reactors. Films of binary and ternary tungsten alloys were synthesized by magnetron sputtering. The oxidation behaviour was measured with a thermobalance set up under synthetic air at temperatures up to 1273 K.
Binary alloys of W-Si showed good self passivation properties by forming a SiO_2 film at the surface. Using ternary alloys the oxidation behaviour could be further improved. A compound of W-Si-Cr showed a reduction of the oxidation rate by a factor of 10^4 at 1273 K.

PACS numbers: 28.52.Fa, 81.15.Cd, 81.65.Rv

1. Introduction

Compared with other materials tungsten (W) has the advantage of very low sputter erosion under bombardment by energetic D, T, He ions and atoms from the plasma. Thus a W-based protection material may provide a wall erosion lifetime of the order of five years which is a pre-requisite for economic fusion reactor operation [1-3].
A potential problem with the use of pure W in a fusion reactor is the formation of radioactive and highly volatile WO_3 compounds and their potential release under accidental conditions. A loss-of-coolant event (LOCA) in a He-cooled reactor would lead to a temperature rise to 1373 K after approx. 10 to 30 days due to the nuclear decay heat of the in-vessel components [1], see also figure 1. In such a situation additional accidental intense air ingress into the reactor vessel would lead to the strong exothermic formation of WO_3 and subsequent evaporation of radioactive $(WO_3)_x$-clusters [4,5].
The use of self passivating W alloys either as bulk material or as thick coating on the steel wall may be an alternative and passively safe for the plasma-facing protection. The use of this material would eliminate the above mentioned concern related to pure W.

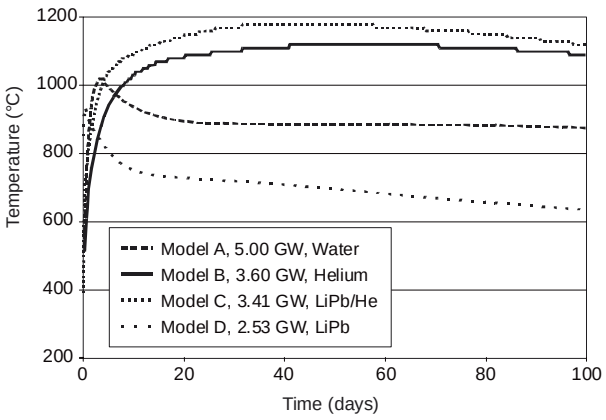

Figure 1. Temperature rise of in-vessel components in a reactor during a loss-of-coolant accident, taken from ref. [1]. Curves show temperature rises for reactors with different coolants used.

2. Experimental

Thin W, W-Si and W-Si-Cr coatings were synthesized and subjected to oxidation at high temperatures to study the self-passivation of the W alloys in comparison to pure W. For this study coatings with µm thickness have been used, because alloys of different composition could be easily deposited using a commercial magnetron sputtering facility. The films are used as model for the oxidation behaviour of bulk materials. The sputter deposition leads to a nanoscale distribution of all elements of the alloy which may be important regarding the diffusion behaviour of the species because of the extremely low diffusion coefficients leading to very short diffusion distances (see e.g. [6]).
The sputter targets were made of pure W (99.5 wt.%), WSi_2 (99.5 %), Si (99.999 %), and Cr (99.95 %), partially produced by powder metallurgy. The deposition was performed on substrates of Inconel LC 713 which is an oxidation resistant high temperature nickel base alloy. Also quartz substrates were used which are fully oxidation resistant and do not react with the W alloys over the investigated temperature range. These two types of coated substrates were used for oxidation tests. Further characterization was carried out on coatings deposited on Si and Graphite substrates. Before the deposition the substrates were cleaned in an ultrasonic bath with isopropanol and water. Directly prior to the deposition the substrate surface was sputter cleaned with Ar ions. The deposition parameters are shown in table 1. Film deposition was onto unheated substrates in DC- and RF-mode up to a coating thickness of approximately 5 µm. The film thickness was controlled by varying of the deposition time. Due to a low base pressure of less than $5x10^{-5}$ Pa the oxygen content of the films was kept below 1% which is the detection limit of the XPS analysis used.

Table 1. Sputter deposition parameter for W, W-Si, and W-Si-Cr films. Target size 7.5 cm, the Ar pressure was set to different values between 0.3 and 1 Pa. Also shown are the corresponding compositions measured by ion beam analysis.

Film	Targets, Power (W)				Composition					
					W		Si		Cr	
	W	WSi_2	Si	Cr	at.%	wt.%	at.%	wt.%	at.%	wt.%
W	500				100	100				
WSi1.7	500		218		90	98	10	1.7		
WSi3	470		387		83	97	17	3		
WSi7	258		387		68	93	32	7		
WSi13	100		273		51	87	49	13		
WSi16		500			45	84	55	16		
WSi18	100		273		41	82	59	18		
WSi10Cr10		500		33	44	80	36	10	20	10

The oxidation experiments of the coatings were carried out in a thermobalance, type Cahn 1000 with a sensitivity of 1 µg for weight change. Synthetic dry air at a pressure of 10^5 Pa was guided through a quartz recipient containing the specimen. Heating up to 1373 K was done by a three-zone furnace, the accuracy of the thermocouple measurement at the sample location is estimated to be ± 10K. The base pressure in the recipient before the start of heating was $<10^{-4}$ Pa. During heating Ar was guided at 100 standard cubic centimetre per minute (sccm) at a pressure of 300 Pa above atmospheric pressure through the recipient. Heating rate was 20 K/min. After reaching steady state at the temperature for the oxidation experiment, 100 sccm of preheated synthetic air was introduced. After the oxidation cooling was performed under flowing Ar. For the evaluation of the oxidation rate only the linear parts of the weight gain curves taken during oxidation were used.

3. Results

3.1 As deposited coatings

The composition of the coatings was measured by Rutherford backscattering analyses on thin coatings (300 nm) deposited on graphite substrates. The results were used to estimate the composition of the thick coatings (1 µm…5 µm) deposited with the identical parameter set on quartz and Inconel substrates. The results are shown in table 1. Using a WSi_2 target a depletion of Si in the deposited film compared to the sputter target has been found. It is ascribed to the higher atomic scattering of Si with

residual gas in the sputter facility and possibly also to different sticking coefficients for W and Si atoms. The density values of the films were close to theoretical densities assuming no formation of other crystalline phases.

XRD analysis of the as deposited W-Si films with low Si concentration showed crystalline phases of α–W and W_5Si_3 (sample with 1.7 wt.% Si). With increasing Si content the sizes of the crystallites become smaller, as seen by the broadening of the reflexes. Figure 2 shows the comparison of the XRD measurements. For the sample with 13 % Si no W_5Si_3 could be detected, the W reflex is very broad and covers the 2-theta values where W_5Si_3 reflexes would be expected.

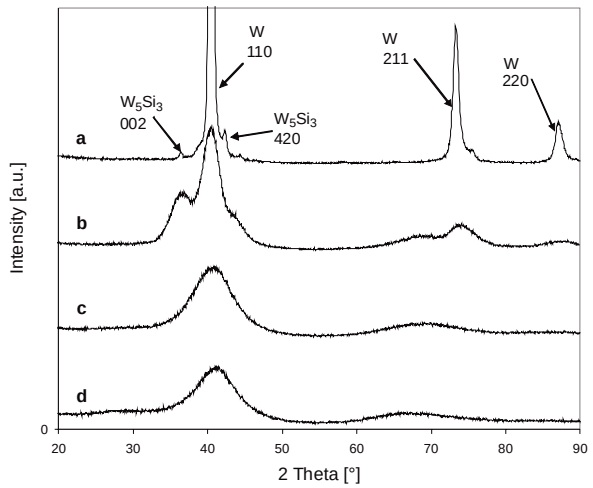

Figure 2. XRD measurements of W-Si films containing (a) 1.7, (b) 3, (c) 7, and (d) 13 wt.% Si.

The results of scanning electron microscopy (SEM) confirm the XRD results. Figure 3a shows the surface of a W-coating with 13 % Si. It shows a very smooth structure according to the small crystallite sizes. A macro particle is shown on the left hand side of the figure. A few of these particles have been found, but are not representative. The sample containing 1.7 % Si (figure 3b) shows a higher roughness, due to the distinct crystallites.
The investigated W-Cr and W-Si-Cr samples were very smooth and showed similarity to the samples of high Si content with no visible structures.

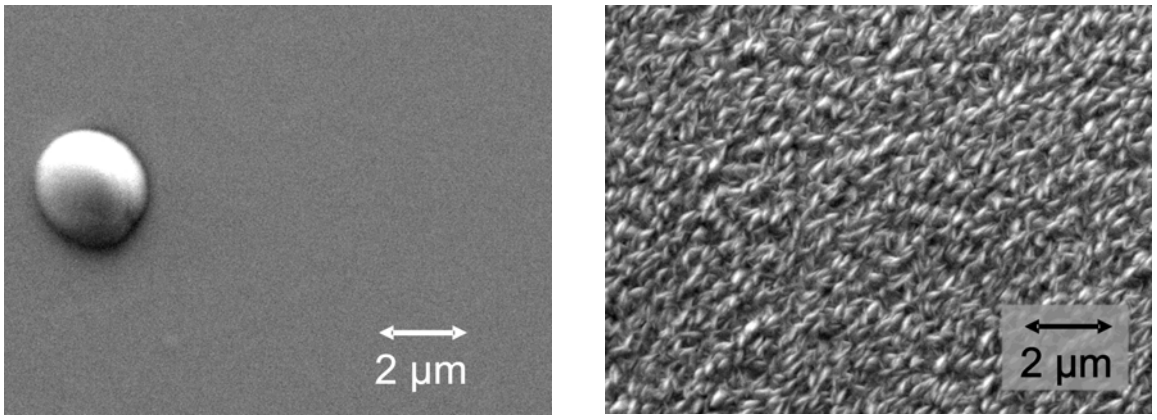

a) b)

Figure 3. SEM surface images of W-Si films, (a) 13 wt.% Si, (b) 1.7wt.% Si.

3.2 Oxidation test results

Self passivation takes place if the system is able to form a dense protecting film at the outer surface. This oxide or nitride film constrains the diffusion of oxygen to the metallic surface and/or the diffusion of the metal to the outer surface of the growing passivating film. The diffusion process through the protecting film will determine the velocity of the oxidation, with increasing thickness of the oxide or nitride scale the oxidation rate will decrease. Thus the weight increase follows a parabolic law. The development of the protective film leads to a depletion of the oxide forming component of the alloy close to the surface. If the concentration becomes too low, e.g. in a thin film, the protecting layer may stop growing. In this case the oxidation characteristic becomes linear. This effect may become evident at relatively short oxidation time already when thin films are used as the model system. Therefore we used a linear fit of the initial phase of the weight increase during oxidation to calculate the oxidation rate. This means that the linear oxidation rates of thin films may be higher than parabolic oxidation rates of a bulk material with the comparable composition.

3.2.1 Tungsten

W-films of 1.5 µm thickness deposited on Inconel have been oxidized at 873, 1073 and 1273 K. Table 2 shows the linear fitted oxidation rates. At 1073 K the oxidation was completed within 5 minutes, no further mass gain was detected. The result was a greenish paper like film. XRD analysis showed only reflexes of WO_3. According to the mass balance the conversion was complete, stoichiometric WO_3 was formed. The activation energy E_a of W oxidation derived from the Arrhenius plot (figure 4) was 80 kJ mol^{-1}. In comparison with literature data, this value is at the lower limit of the published data. There is considerable scatter, however. In addition, our data have been obtained from sputtered thin films, while most literature data were measured on bulk tungsten samples.

Table 2. Linear oxidation rates of pure tungsten and tungsten-silicon alloys containing 1.7, 3, 13, and 18 wt.% silicon.

	Linear oxidation rate (mg cm^{-2} s^{-1})		
	873 K	1073 K	1273 K
W	$4.5\ 10^{-4}$	$4.7\ 10^{-3}$	$1.4\ 10^{-2}$
WSi1.7	$4.8\ 10^{-5}$	$1.3\ 10^{-3}$	$9.1\ 10^{-3}$
WSi3	$1.4\ 10^{-4}$	$5.4\ 10^{-4}$	$5.0\ 10^{-3}$
WSi13	$1.0\ 10^{-5}$	$3.1\ 10^{-4}$	$2.3\ 10^{-3}$
WSi18	$7.0\ 10^{-6}$	$5.0\ 10^{-5}$	$1.3\ 10^{-3}$

Regarding the kinetics of the oxidation processes on pure W, at low oxidation temperatures an initial WO_2 film might form. However, the diffusion of oxygen through this layer is rapid and continued fast oxidation of the W takes place. On pure W the oxidation at low temperatures may follow a parabolic law [7]. At higher temperatures (here 873, 1073 and 1273 K) WO_3 will form which will not grow as a dense layer and thus WO_3 will not protect the W surface from oxygen contact.

3.2.2 W-Si alloys

In the system W-Si-O SiO_2 is the thermodynamically most stable component, and thus W-Si compounds will form SiO_2 as the final stable oxidation product. Free Si, W_5Si_3 and WSi_2 will directly form SiO_2. W oxides would be directly reduced by the excess of Si to SiO_2 and W. Thus in the case of Si containing compounds a protective and dense SiO_2 layer will be formed which acts as a diffusion barrier. Oxygen has to diffuse through this barrier layer and as a result the oxidation rate follows a parabolic law with time. The oxidation behaviour of the W-Si alloys was investigated on quartz as well as on Inconel substrates. Particularly at high temperatures the oxidation rates of the layers deposited on Inconel substrates showed strongly reduced values compared to those on quartz. Also the characteristic of the weight gain was different. For the Inconel samples the decreasing of the oxidation

rate by time was very pronounced. Presumably the substrates influenced the oxidation behaviour by diffusion of Ni to the W-Si system which supported the formation of barrier layers with Ni oxides. The quartz samples did not show any influence to the investigated system, therefore only quartz samples were used for further oxidation experiments. However, addition of Ni to the system W-Si may be promising and will be the subject of later investigations.

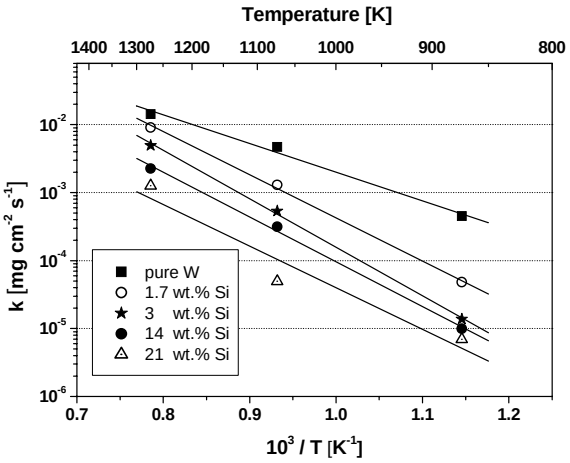

Figure 4. Arrhenius plot of oxidation rates of pure tungsten and W-Si alloys with 1.7, 3, 13, and 18wt.% silicon.

The oxidation rate of W-Si alloys depends on the content of Si. Increasing Si content decreases the oxidation rate. A comparison of the oxidation rates of pure tungsten and W-Si alloys with 1.7, 3, 13, and 18 wt.% silicon is presented in table 2. The activation energies of the W-Si compounds vary between 117 and 136 kJ mol^{-1} (figure 4). These values are clearly higher than E_a of pure W layers (80 kJ mol^{-1}). They are in the order of the activation energy of silicon, which is a diffusion controlled oxidation [8]. The oxidizing species diffuse through the oxide film to the interface. A dependence of E_a on the Si content was not found.
SEM images (figure 5) show a sample of W-13wt.%Si after oxidation at 1073 K for 4 hours. The conversion of Si to SiO_2 and of W to WO_3 was not completed after that time. The light grey areas of image 5a have an oxygen content of 12 at.% according to EDX analysis. Taking the information on the depth of the EDX analysis into account we interpret the light grey area as the domain of the sample where the alloy is protected by a thin film of SiO_2. By contrast the oxygen content of the dark areas is about 62 at.%, which we interpret in the following way: With increasing oxidation time the SiO_2 scale is growing and the content of Si in the alloy layer becomes lower, tungsten starts to oxidize with high increase of volume. This may locally damage the protecting SiO_2 layer. The full oxidation of W starts at this nucleation site, the total oxidized areas grow radially from this nucleation sites. It formed the dark circles which have been grown together. They cover a large part of the surface. Figure 5b shows the marked detail of the surface of image 5a demonstrating a volume increase of the strongly oxidized zones. The oxygen content of this area reflects the nearly complete conversion of W and Si to their oxides, which can explain the high oxygen content in these dark areas. Possible origin of such nucleation sites for increased oxidation may be microscopic voids in the coating e.g. pinholes, embedded micro particles or substrate inhomogeneities.

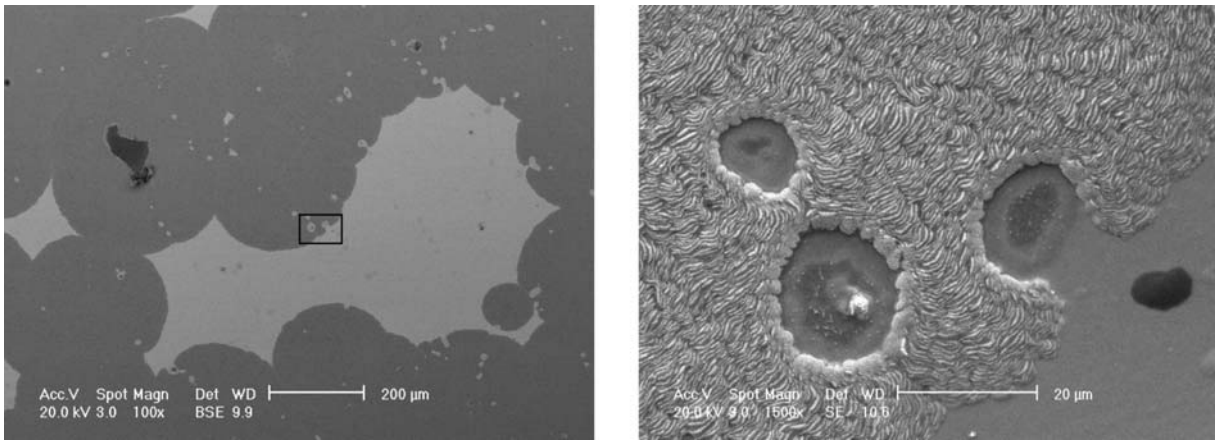

a) b)

Figure 5. SEM plan view of 1 µm WSi13 oxidized at 1073 K for 4 hours. The light grey areas of image (a) have a low oxygen content according to EDX analysis. The oxygen content of the dark area is about 62 at.%. Image (b) shows the marked detail of the left.

3.2.3 W-Si-Cr alloys

Under an oxidizing atmosphere a ternary alloy should form a stack of different oxides as a protecting system. Depending on the thermodynamics of the oxidation process and the diffusion properties of the involved elements a sequence of the different oxide layers will be built up and may enhance the protecting properties [9]. The protective layers in the W-Si-Cr system will be SiO_2 and Cr_2O_3. Compared to the W-Si system the addition of chromium was advantageous. The oxidation rates could be further decreased by formation of the additional Cr_2O_3 layer. Figure 6 shows XPS depth profiles of a 1.5 µm thick layer of WSi10Cr10 after oxidation for 22 hours at (a) 873 K and (b) 1073 K. The depth profiles were performed by sputtering with Ar ions, the time scale corresponds to some ten nanometres. At 873 K the outer surface was only partly oxidized, a thin zone with increased oxygen and silicon content suggests the formation of a SiO_2 layer at the surface. The oxide scale of the sample oxidized at 1073 K is much thicker. The outer surface may consist of Cr_2O_3, but in the depth of the coating the concentration of chromium is strongly reduced. As described before, the concentration of the alloying elements of the coating decreases with increasing oxidation time. Both samples have endured the oxidation without damage, but a sample oxidized at 1273 K failed. The W-Si-Cr layer was partly delaminated from the substrate during the oxidation experiment.

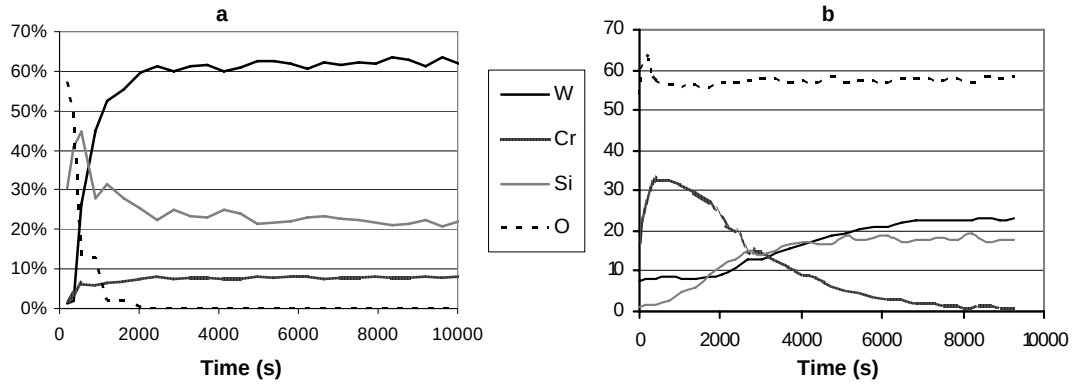

Figure 6. XPS composition depth profile of 1.5 µm coatings of WSi10Cr10 oxidized at (a) 873 K and (b) 1073 K for 22 h. The depth profiles were obtained by sputtering with Ar ions, the time scale corresponds to some ten nanometers.

If self passivation cannot continue with progressing oxidation time due to the lack of alloying elements, the full oxidation of W starts like described for the W-Si system. But the behaviour of the two systems is different. In case of W-Si the growing WO_3 shows good adhesion, whereas the coating starts to delaminate in case of W-Si-Cr. Figure 7 shows delamination on a 2.5 µm thick WSi10Cr10 film, oxidized for 4 hours at 1073 K.

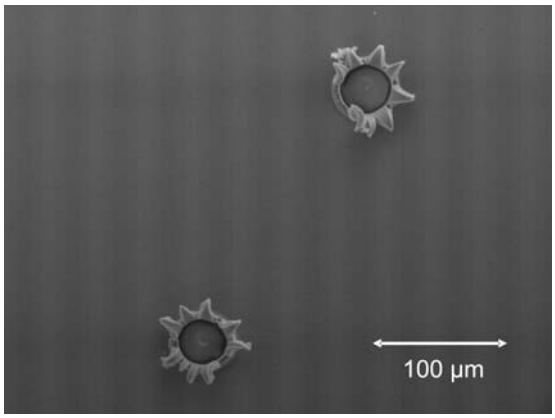

Figure 7. SEM surface image of 2.5 µm WSi10Cr10 oxidized for 4 h at 1073 K.

To reduce the depletion of chromium from the bulk alloy during the oxidation process, the thickness of the WSi10Cr10 layer was varied. A 4.6 µm thick coating survived 22 hours at 1273 K without any delamination, the oxidation rate was $1.9 \cdot 10^{-6}$ mg cm^{-1} s^{-1}. Compared to the W-Si samples the oxidation rate was further dramatically reduced. Figure 8 compares the oxidation rates of tungsten, WSi18, and WSi10Cr10 at different temperatures.

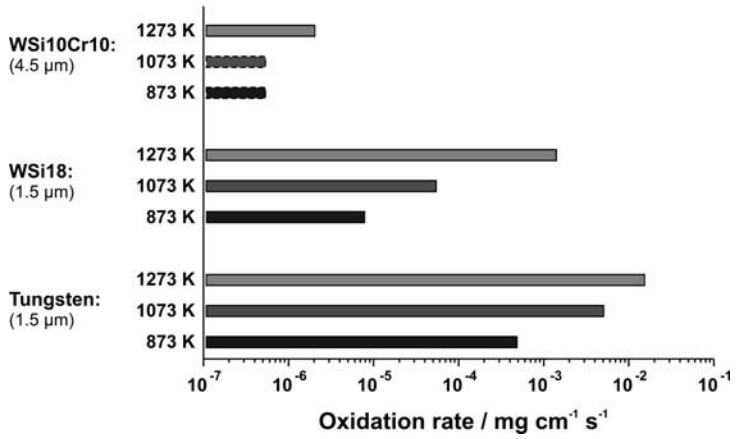

Figure 8. Oxidation rates of pure W, WSi18 and WSi10Cr10 in synthetic air (1 bar).

4. Conclusion

The self-passivation mechanism of substoichiometric W-Si compounds and of W-Si-Cr alloys under oxidation has been shown.

A future application of W-Si or W-Si-Cr alloys in a fusion reactor appears feasible, since these compounds can also be processed to thick protective coatings with reasonable thermal conductivity, e.g. by plasma spraying with subsequent densification. Enhanced sputter erosion during normal reactor operation due to the Si and Cr addition is not a concern, since preferential sputtering of Si and Cr will lead to rapid depletion of the first atomic layers and leave a pure W-surface in contact with the plasma [10]. In case of an accidental temperature rise under LOCA conditions the diffusion of Si and Cr in W will lead to the enrichment of oxide scale forming elements at the surface which is needed for the formation of a passivating dense oxide layer.

Acknowledgement
A part of this work has been performed within the framework of the Integrated European Project "ExtreMat" (contract NMP-CT-2004-500253) with financial support by the European Community. It only reflects the view of the authors and the European Community is not liable for the use of the information contained therein.

References

[1] Maisonnier D et al 2005 *A Conceptual Study of Commercial Fusion Power Plants; Final Report of the European Fusion Power Plant Conceptual Study (PPCS)* EFDA-RP-RE-5.0
[2] Bolt H, Barabash V, Federici G, Linke J, Loarte A, Roth J and Sato K 2002 *J. Nucl. Mater.* **307-311** 43-52
[3] Federici G et al 2001 *Nuclear Fusion* **41** 1967
[4] Smithells C J 1983 *Metals Reference Book, 6th Ed.* London Butterworth
[5] Yang Y A, Ma Y, Yao J N and Loo B H 2000 *J. of Non-Crystalline Solids* **272** 71-74
[6] Landolt-Börnstein 1990 *Numerical Data and Functional Relationship in Science and Technology, New Series* Volume 26 Springer
[7] Lassner E and Schubert W 1999 *Tungsten: Properties, Chemistry, Technology of the Element, Alloys, and Chemical Compounds* New York Kluwer Academic
[8] Doremus R H 1976 *J. of Physical Chemistry* **80 (16)** 1773
[9] Stergiou A, Tsakiropoulos P and Brown A 1997 *Intermetallics* **5 (1)** 69-81
[10] Eckstein W et al 2001 *Atomic and Plasma-Material Interaction Data for Fusion* **7b** (IAEA, Vienna) 76